SiO2–Na2O–B2O3 density: A comparison of experiments, simulations, and theory

Marina Barlet, Ali Kerrache, Jean-Marc Delaye, Cindy L. Rountree

SiO₂–Na₂O–B₂O₃ density: A comparison of experiments, simulations, and theory

Marina Barlet [a], Ali Kerrache [b], Jean-Marc Delaye [b], Cindy L. Rountree [a],*

[a] CEA, IRAMIS, SPCSI, Groupe Complex Systems & Fracture, F91191 Gif-sur-Yvette, France
[b] CEA, DEN, DTCD, SECM, LMPA CEA Marcoule, BP 17171, 30207 Bagnols sur Cèze cedex, France

ARTICLE INFO

ABSTRACT

This paper is devoted to a comparison of experimental, simulation, and theoretical results on the density of SiO₂–B₂O₃–Na₂O glasses. It is found that theoretical and simulation densities do compare favorably with experimental values yet simulations give a better estimate of the density of the samples. Furthermore, the structural make-up (i.e. types of borate and silicate units) of the ternary glasses and the volume of the elementary units have also been investigated with simulations and compared to theory. These results are found to compare favorably when $R < R_{d1}$ $\left(R = \frac{[Na_2O]}{[B_2O_3]}, K = \frac{[SiO_2]}{[B_2O_3]} \right.$ and $\left. R_{d1} = 0.5 + 0.25K \right)$ yet variations do exists when $R > R_{d1}$. These variations include more Na⁺ ions attaching to the borate network in simulations than theorized.

© 2013 Elsevier B.V. All rights reserved.

1. Introduction

Sodium oxide (Na₂O), boron trioxide (B₂O₃), and silica (SiO₂) are the three major components of many industrial important glasses including: BOROFLOAT 33, Schott BK-7 Borosilicate Crown Glass, Corning Pyrex 7740 …. The uses of these glasses range from cookware to laboratory glassware to optical glass. Due to the varying applications, many studies have been conducted to understand how the molar mass of each component affects the ternary glass structure. These studies include several spectroscopic techniques such as Raman [1–3], Infrared [4], NMR [5,6] …. Moreover, NMR measurements permit quantitative structural information by employing ¹¹B NMR [7–10] and ²⁹Si NMR [11]. Subsequent studies suggest that the structural building blocks can be used to predict the densities of the ternary glasses [12–14]. A disadvantage to the structural building block models is that they are strictly based on least-square data fits.

Understanding the structural makeup of these glasses is by far more complicated than the previous papers imply. Thus experiments are used to investigate the density of seven ternary glass systems. In addition, molecular dynamics (MD) simulations are used to gather information on the fraction and volume of elementary building blocks and the overall densities of these systems. These results are compared and contrasted to other models and data acquired herein and from literature (compiled in Appendix A).

This paper will first present a review of the structural makeup of the SiO₂–B₂O₃–Na₂O ternary glasses. In developing this section, the coauthors have scoured the current literature. All of the parts of the picture exist in literature, yet the comprehensive picture we are trying to bring has been alluded to but never realized. Section 3 depicts how the fractions of the structural units are used to estimate the densities of glasses in several models. The next two sections detail our experimental and simulation procedures. Afterwards is a presentation of the experimental and simulation results and how they compare and contrast with current theories.

2. Review of structural makeup

In general, ternary glass structures are complex glasses whose structure is dependent on its oxides and their relative proportion. Herein sodium borosilicate ternary glasses are composed of two network formers (SiO₂ and B₂O₃) and one network modifier (Na₂O) [15–17]. Pure silica (amorphous SiO₂) and pure boron trioxide form an amorphous network with no long range order. Despite the lack of long range order both silica and boron trioxide have short- and mid-range orders. The short range order of silica is a tetrahedron (SiO₄) and four bridging oxygen atoms. The mid-range order is the linking of the tetrahedrons to form predominantly 6-membered rings (number of silicon per ring) with some ring size dispersions [18–23]. Similarly, B₂O₃ has a mid-range order of boroxol rings (3 borons per ring) [24–26]. B₂O₃'s short range order is a planar BO₃/₂ group and has no non-bridging oxygen atoms (NBOs). (Borons with 3 bridging oxygen atoms attached to it shall be referred to as B3 henceforth.) Contrary to SiO₂ and B₂O₃, Na₂O is an antifluorite crystal structure. Mixing two (i.e. binary glass) or all three components of the glass will lead to variations in the structure of the glasses as reviewed below.

* Corresponding author.
  E-mail address: cindy.rountree@cea.fr (C.L. Rountree).

2.1. Binary B_2O_3–Na_2O glass

The structure of the binary B_2O_3–Na_2O glass has been studied intensively over the past 60 years [10,12,27–30]. The binary B_2O_3–Na_2O structure has 5 well known structural units. The fraction of these units depends on the ratio $R = [Na_2O] / [B_2O_3]$ where $[\cdot] \equiv mol\%$ [8,31]. As stated above a pure B_2O_3 glass has a short-range B3 structure and mid-range structure of boroxol rings. Low quantities of Na_2O (0–20%) added to the B_2O_3 glass will predominantly convert B3 to a tetrahedral BO_4 structure (to be referred to as B4, boron with 4 bridging oxygen atoms) with an adjacent sodium ion forming Tetraborate units (chemical formula $Na_2O \cdot 4B_2O_3$) [8,32]. Additional sodium (20%–33%; $0.25 < R \lesssim 0.5$) will convert Tetraborate units into a diborate group (chemical formula $Na_2O \cdot 2B_2O_3$)). Less frequently at low R, Na_2O can also convert B3s to form planar $BO_{3/2}$ groups each with 1 NBO (non-bridging oxygen) and 1 Na^+ ion nearby (i.e. 2 Metaborate units, chemical formula $(Na_2O \cdot B_2O_3)$) [12]. However this conversion is rare and frequently ignored. Locally all $R < 0.5$ conversions correspond to $R_l = 1$ (local conversion ratio implying one Na^+ ion for the borate unit). For $R > 0.5$, other structural units will come about including: (1) Metaborate units: a planar $BO_{3/2}$ group with 1 NBO and 1 Na^+ ion nearby (chemical formula $(Na_2O \cdot B_2O_3)$ and local $R_l = 1$); (2) Pyroborate unit: a planar $BO_{3/2}$ group with 2 NBOs and 2 Na^+ ions nearby (chemical formula $\frac{1}{2}(2Na_2O \cdot B_2O_3)$ and local $R_l = 2$); (3) orthoborate unit: a planar $BO_{3/2}$ group with 3 NBOs and 3 Na^+ ions nearby $\frac{1}{2}(3Na_2O \cdot B_2O_3)$ and local $R_l = 3$; and (4) "loose" B3 and B4 units: B3 and B4 units which are not part of any other structure but maintain all of their bridging oxygen atoms [10,12,27–30].

As stated above, the fractions of structural units are dependent on the molar mass. Frequently fractions are noted by f_i where i ranges from 1 to 5. The groups correspond as follows:

- f_1: the fraction of planar $BO_{3/2}$ group with all bridging oxygen atoms (Fig. 1a)
- f_2: the fraction of BO_4 tetrahedra with all bridging oxygen atoms (Fig. 1b)
- f_3: the fraction of planar $BO_{3/2}$ groups with 1 NBO and 2 bridging oxygen atoms (Metaborate; Fig. 1c)
- f_4: the fraction of 3-coordinated boron with 2 NBOs and 1 bridging oxygen atom (Pyroborate; Fig. 1d)
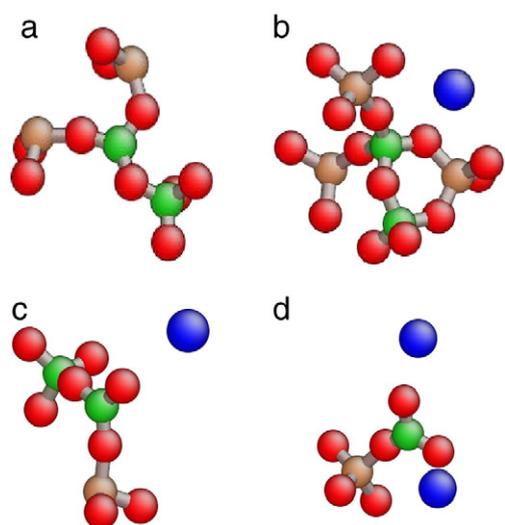- f_5: the fraction of 3-coordinated boron with 3 NBOs (orthoborate unit — this group is frequently negligible)

For the case of low quantities of sodium ($R < 0.5$), Yun and Bray found that the glass structure is predominantly a mixture of planar $BO_{3/2}$ groups and BO_4 tetrahedra [7–10] and the Metaborate, Pyroborate, and orthoborate groups are considered negligible. The fraction of B4 units, f_2, was found to be $.95R$ [8] experimentally and structural models conjectured f_2 to be R [32]. Considering experimental uncertainties these results compare favorably. Subsequent models are based on $f_2 = R$ for $R < 0.5$. Thus, the fractions of each are estimated as follows:

$$\left.\begin{array}{l} f_1 = 1 - R \\ f_2 = R \\ f_3 = 0 \\ f_4 = 0 \end{array}\right\} R < 0.5. \tag{1}$$

The creation of BO_4 tetrahedra leads to the annihilation of planar $BO_{3/2}$ groups. The continual addition of sodium to the binary B_2O_3–Na_2O system is just a special case of the ternary SiO_2–B_2O_3–Na_2O glass (which is detailed in Subsection 2.4). For high levels ($R \gtrsim 0.8$) of sodium $[Na_2O] \gtrsim 45\%$ and $[B_2O_3] \lesssim 55\%$, the binary B_2O_3–Na_2O system is no longer amorphous [33]. Yet the equations of Subsection 2.4 give a reasonable estimate of the densities (presented in Section 3).

2.2. Binary Na_2O–SiO_2 glass

The binary Na_2O–SiO_2 glass structure has been studied via ^{29}Si MAS (magic-angle spinning) NMR measurements and Raman spectroscopy [12,34–39]. Five structural units are known to exist in this system, and they are dependent on the molar ratios of Na_2O to SiO_2 ($J = [Na_2O]/[SiO_2]$). Frequently fractions are noted by Q_i where i ranges from 0 to 4. The groups correspond as follows:

- Q_4: the fraction of SiO_4 tetrahedrons with all bridging oxygen atoms
- Q_3: the fraction of SiO_4 tetrahedrons with 1 NBO and 3 bridging oxygen atoms
- Q_2: the fraction of SiO_4 tetrahedrons with 2 NBOs and 2 bridging oxygen atoms
- Q_1: the fraction of SiO_4 tetrahedrons with 3 NBOs and 1 bridging oxygen
- Q_0: the fraction of SiO_4 tetrahedrons with 4 NBOs and 0 bridging oxygen atom.

Many authors use the lever rule [13,12] or Gaussian fits to estimate Q_i [14,40]. Analyzing data in Maekawa et al.'s paper neither gives a sufficient estimate alone [40]. Moreover a Gaussian fit is not rational for Q_0 when it ideally should migrate to 1. Thus the following equations will be adopted to describe the Q_i fractions:

$$Q_4 = \begin{cases} -2J + 1 & J \le .25 \\ A_4 e^{-\left(\frac{2J - B_4}{C_4}\right)^2} & J > .25 \end{cases}$$

$$Q_3 = \begin{cases} 2J & J \le .25 \\ A_3 e^{-\left(\frac{2J - B_3}{C_3}\right)^2} & J > .25 \end{cases} \tag{2}$$

$$Q_i = A_i e^{-\left(\frac{2J - B_i}{C_i}\right)^2} \quad \text{for } i = 2 \text{ or } 1$$

$$Q_0 = \frac{1}{1 + 2.2*10^5 e^{-3.65*(2J)}}$$

[40] where A_i, B_i, and C_i are the coefficients for the Gaussian fits (Table 1). Details of how these equations are arrived at are presented in Appendix B. The formation of NBO actually leads to a secondary effect corresponding to a change in the volume. In the context of the silica tetrahedral structure, the variations which occur are: (1) the bond length between Si–NBO is less than 1.62 Å (i.e. the length between Si–O atoms in pure silica), and (2) the bond length between Si and bridging oxygen atoms increases [41,42]. Experiments (neutron and x-ray

Fig. 1. The images depict the main borate structures: a) f_1; b) f_2; c) f_3; and d) f_4. The color code is: B — green; Si — orange; O — red; and Na — blue.

diffraction combined with reverse Monte Carlo methods) reveal a shift in the ring sizes from 6 membered to an average of 7.6 membered rings in 70-SiO_2/30-Na_2O glass [43]. More Na_2O will further increase the ring structure size as shown by Du and Cormack [44].

2.3. Binary SiO_2–B_2O_3 glass

Out of the three binary glasses systems the SiO_2–B_2O_3 glass system has been studied the least over the years yet still some work has been done [39,45–47]. Boron atoms are three-coordinated and independent of the B_2O_3 content, and silicon atoms are four-coordinated. The interconnection of the two networks (i.e. proportion of Si–Si, B–B, and Si–B connections) is important to the density measurements because the bond lengths between the Si–Si (~3.06 Å), B–B (~2.69 Å), and Si–B (~2.80 Å) connections are not equivalent [48]. Nevertheless, the amount of intermixing between the two networks is still an open question [39,45–47]. Thus more experimental research is needed to conclusively tell the structure, and this is a subject outside of the scope of this paper.

2.4. Ternary SiO_2–B_2O_3–Na_2O glass

SiO_2–B_2O_3–Na_2O glass systems have been studied quite extensively over the years [4,10,12,28,29,49,50]. In the late 1970's and early 1980's Dell et al. published a series of papers [10,28,29] on how the addition of sodium to binary SiO_2–B_2O_3 glass modifies the structural units of the system. Again we will use the nomenclature presented above. As presented by Feil and Feller [13], the initial addition of sodium to a binary SiO_2–B_2O_3 glass leads to the creation of BO_4 tetrahedrons and the annihilation of a planar $BO_{3/2}$ group system. It is conjectured that the structure being formed during this transformation is a diborate group (2 4-coordinated borons and 2 3-coordinated borons with zero NBO). During this process the silica network remains undisturbed. Implying, the number of NBO, $f(Si_{NBO})$, on silica tetrahedrons is zero. This process continues until $R = 0.5$. Subsequently between $R = 0.5$ and $R_{max} = 0.5 + \frac{1}{16}K$ reedmergnerite units appear. Reedmergnerite units contain one four-coordinated boron bonded to 4 silica tetrahedrons (chemical composition: $\frac{1}{2}(Na_2O \cdot B_2O_3 \cdot 8SiO_2)$) [29,51]. Otherwise the silica network remains fully coordinated with no NBO. Thus, the fractions between $R = 0$ and R_{max} are estimated as follows [10,13,14,28,29]:

$$\left. \begin{array}{r} f_1 = 1-R \\ f_2 = R \\ f_3 = 0 \\ f_4 = 0 \\ f(Si_{NBO}) = 0 \end{array} \right\} 0 < R < R_{max}. \qquad (3)$$

Beyond this point, additional sodium goes to the formation of NBO on silica units in reedmergnerite groups. This transformation is proposed to be valid until $R_{d1} = 0.5 + 0.25K$. Thus, the fractions of each are estimated as follows [10,13,14,28,29]:

$$\left. \begin{array}{r} f_1 = 1-R_{max} \\ f_2 = R_{max} \\ f_3 = 0 \\ f_4 = 0 \\ f(Si_{NBO}) = \dfrac{2(R-R_{max})}{K} \end{array} \right\} R_{max} < R < R_{d1}. \qquad (4)$$

Subsequent molecules of Na_2O are shared between the diborate and reedmergnerite units and the formation of NBO on silica tetrahedrons. During this process diborate units are transformed into pyroborate units (1 3-coordinated boron with 2 NBOs) at a rate of $(2-0.25\,K)/(2 + K)$. Reedmergnerite units are transformed into pyroborate units and silica tetrahedrons with 2 NBOs per Si atom at a rate of $(K + 0.25\,K)/(2 + K)$. This process continues until all 3-coordinated

borons contain at least 1 NBO (i.e. $f_1 = 0$) or $R_{d2} = 1.5 + .75\,K$. Thus, the fractions of each are estimated as follows [10,13,14,28,29]:

$$\left. \begin{array}{r} f_1 = \dfrac{(8-K)}{8} * \left(.75 - \dfrac{R}{2+K}\right) \\ f_2 = \dfrac{(8+K)}{12} * \left(1 - \dfrac{R}{2+K}\right) \\ f_3 = \dfrac{(R-R_{1d})}{12} * \dfrac{(8-K)}{(2+K)} \\ f_4 = \dfrac{(R-R_{1d})}{8} * \dfrac{(8-K)}{(2+K)} + \dfrac{K}{6}\left(\dfrac{R}{(2+K)} - .25\right) \\ f(Si_{NBO}) = \dfrac{3}{8} + \dfrac{13}{6}\left(\dfrac{R-R_{1d}}{2+K}\right) \end{array} \right\} R_{1d} < R < R_{d2}. \qquad (5)$$

This process continues until all borate units are classified as pyroborate units (f_4) and all silica units are free (i.e. no bridging oxygen atoms). Thus, the fractions of each are estimated as follows [10,13,14,28,29]:

$$\left. \begin{array}{r} f_1 = 0 \\ f_2 = \dfrac{(8+K)}{12} * \left(1 - \dfrac{R}{2+K}\right) \\ f_3 = \dfrac{1}{6}(8-K) * \left(1 - \dfrac{R}{2+K}\right) \\ f_4 = \dfrac{(8-K)}{16} + \dfrac{(R-R_{2d})}{4} * \left(\dfrac{8-K}{2+K}\right) + \dfrac{K}{6}\left(\dfrac{R}{2+K} - 0.25\right) \\ f(Si_{NBO}) = \dfrac{3}{8} + \dfrac{13}{6}\left(\dfrac{R-R_{1d}}{2+K}\right) \end{array} \right\} R_{d2} < R < R_{d3} \qquad (6)$$

where $R_{d3} = 2 + K$. Based on Eq. (6) after R_{d3}, the fractions can be estimated as follow:

$$\left. \begin{array}{r} f_1 = f_2 = f_3 = 0 \\ f_4 = 1 \\ f(Si_{NBO}) = 2 \end{array} \right\} R_{d3} < R. \qquad (7)$$

Hence the silicate and borate structures are considered not to evolve. However, one would assume that f_5 units (orthoborate units) are formed in this region, but not much research currently exists to display the fraction of the system which should be devoted to f_5. This is outside the scope of this paper, thus we will ignore the orthoborate units like our predecessors.

Over the past 20 years, the validity of these fractions has been questioned [31,39,49,52–54]. One of the most interesting, and relevant, is the mixing of the borate and silicate phases as stated in Subsection 2.3. The fractions do not take this into consideration. Recent studies have tried to better model the mixing of the phases [31], yet it is difficult to model with current experimental data.

3. Review of density estimates knowing K and R

Feil and Feller [13] proposed an equation to extract the density knowing K and R and the fraction of borate units. They proposed

$$\rho = \frac{M_1 f_1 + M_2 f_2 + M_3 f_3 + M_4 f_4 + \dfrac{K}{2}M'}{V_1 f_1 + V_2 f_2 + V_3 f_3 + V_4 f_4 + \dfrac{K}{2}V'} \qquad (8)$$

Table 1
Coefficients for Gaussian fits maintain continuity Q_i and are within the bounds of the best fits' 95% confidence bounds.

	A	B	C
Q_4	1.04	−0.19	0.8
Q_3	.77	1.02	0.79
Q_2	.71 ± .04	2.08 ± .04	0.79 ± .05
Q_1	.52 ± .05	2.94 ± .05	.8

Table 2
Molar volume of borate and silicate units extracted from various different theories. Values for pure B_2O_3 and pure SiO_2 are arrived at by: (1) averaging volumes found in literature and (2) assuming the full system is dedicated to f_1 and Q_i respectively (implying no NBO). Feil and Feller [13] and Budhwani and Feller [12] reported reduced units. Herein they have been converted to real values for comparison. These values are to be used to calculate density measurements.

Reference	Borate units				Silicate units				
	V_1	V_2	V_3	V_4	V'_4	V'_3	V'_2	V'_1	V'_0
Pure silica $\rho = 2.212$	0	0	0	0	27.16	0	0	0	0
Pure B_2O_3 $\rho = 1.824$	19.08	0	0	0	0	0	0	0	0
Feil and Feller [13]	19.1	23.9	30.9	40.9	Not applicable (na); Eq. (11)				
Budhwani and Feller [12]	19.1	23.9	30.9	40.9	na; Eq. (12)				
Inoue et al. [14] (cm³/ mol)	19.2	21.0	29.0	41.7	26.3	35.2	50.3	20.8	na

where M_i (where i varies from 1 to 4) corresponds to the mass of the borate structural units and are text book values:

$$M_1 = M_B + 1.5 * M_O$$
$$M_2 = M_3 = M_B + 2 * M_O + M_{Na} \quad (9)$$
$$M_4 = M_B + 2.5 * M_O + 2 * M_{Na}$$

where M corresponds to the masses of the atoms specified. V_i (where i varies from 1 to 4) corresponds to the volume of the borate structural units. Feil and Feller derived these values from the least square fits of density measurements. There values are reported in Table 2. M' and V' correspond to the mass and volume of silica tetrahedral units, respectively. M' is calculated as follows:

$$M' = M_{Si} + (2 + 0.5 * f(Si_{NBO}))M_O + f(Si_{NBO})M_{Na} \quad (10)$$

where M corresponds to the masses of the atoms specified. The factor ½ arises because K is inversely proportional to B_2O_3 rather than $BO_{3/2}$. To acquire V', Feil and Feller applied a least square fit to Eq. (8) giving:

$$V' = 25.2 + 10.5 * f(Si_{NBO}). \quad (11)$$

Fig. 2 (left) depicts Feil and Feller's fit in 3D and data points measured herein and acquired from literature (Appendix A). For ease of comparing, Fig. 2 (right) depicts the % error. Negative values correspond to an under estimate of the fits. Values of interest herein (percent of silica and boron ranging from 43% to 70% and 14.5% to 29% respectively) are consistently underestimated. The average error in the region of interest is 1.6% with a maximum error of 4.4%. Moreover, it should be noted that

the density of pure silica using this equation is approximately 8% higher than the accepted value (2.38 g/cm³ versus 2.20 g/cm³).

Budhwani and Feller [12] modified Feil and Feller's volume to a slightly more complicated volume term:

$$V' = 27.3 + \begin{cases} 4.58 * f(Si_{NBO}) & f(Si_{NBO}) < 1 \\ 4.58 + 6.68 * (f(Si_{NBO}) - 1) & 1 \le f(Si_{NBO}) \le 2 \end{cases}. \quad (12)$$

These results lead to slightly different values in the density estimate. However, values of interest herein are consistently underestimated. The average error in the region of interest is 4.5% with a maximum error of 7.5%.

Recently, Inoue et al. proposed a new equation to calculate the density [14]. They invoke the first-order mixture model on all components:

$$\rho = \frac{2 * [B_2O_3] \sum f_i M_i + [SiO_2] \sum Q_i M'_i}{2 * [B_2O_3] \sum f_i V_i + [SiO_2] \sum Q_i V'_i} \quad (13)$$

where ρ is the density of the glass of interest. f_i and Q_i are the mole fractions of the ith component of the borate and silicate (respectively) units. Boron units are computed via Eqs. (3)–(7). Silica units are computed as if the system is a binary Na_2O–SiO_2 glass. Thus equations in are evoked with $J = 0.5 f(Si_{NBO})$ where $f(Si_{NBO})$ is defined via Eqs. (3)–(7). The half difference comes from 2 Na^+ ions per silicon atom. M_i and M'_i are the molar masses of the ith component of the borate and silicate (respectively) units. More specifically, M_i is defined as in Eq. (9) and M'_i as below

$$M'_4 = M_{Si} + 2 * M_O$$
$$M'_3 = M_{Si} + 2.5 * M_O + M_{Na}$$
$$M'_2 = M_{Si} + 3 * M_O + 2 * M_{Na} \quad (14)$$
$$M'_1 = M_{Si} + 3.5 * M_O + 3 * M_{Na}$$
$$M'_0 = M_{Si} + 4 * M_O + 4 * M_{Na}$$

V_i and V'_i are the volumes of the ith component of the borate and silicate (respectively) units. To acquire V_i, Inoue et al. have fitted data found in a database [14]. In general, when comparing Figs. 2 (right) and 3 (right) Inoue's fit does give a better estimate of the density. However, the values of interest herein are consistently underestimated. The average error in the region of interest is approximately 0.9% with a maximum error of 4.4%.
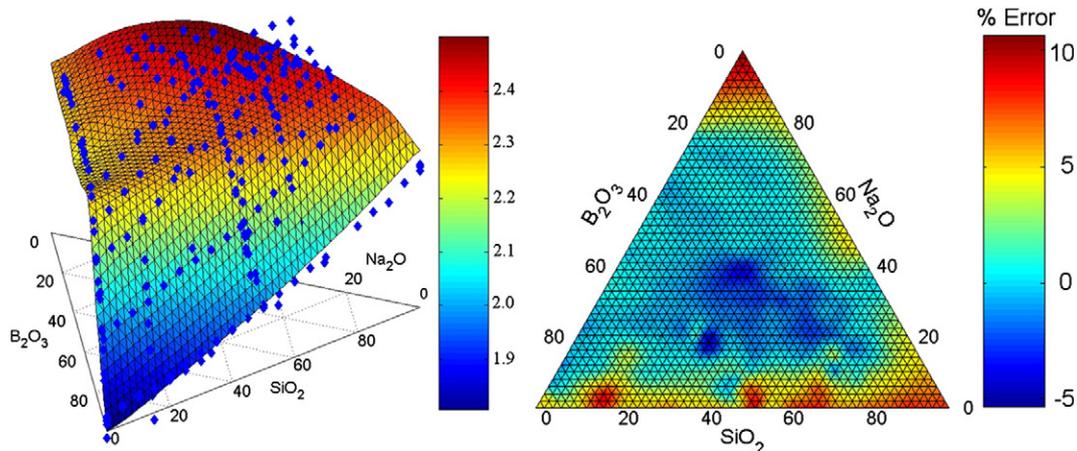
Fig. 2. (Left) Feil and Feller's fit compared with data (blue diamonds) found in literature (collected in Appendix A). (Right) % error when comparing experimental data to Feil and Feller's fit. Positive % errors imply that the fit overestimates data.
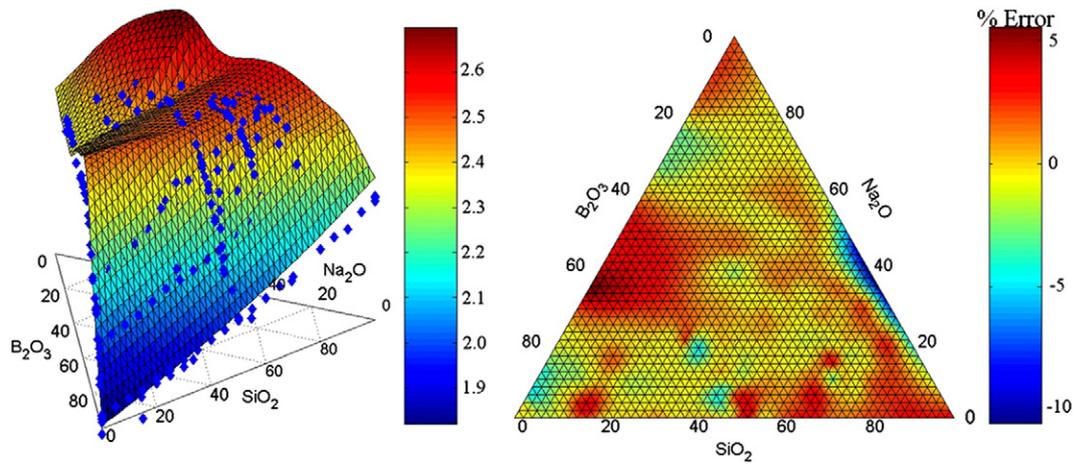
Fig. 3. (Left) Inoue et al.'s fit compared with data (blue diamonds) found in literature (collected in Appendix A). (Right) % error when comparing experimental data to Inoue's fit. Positive % errors imply that the fit overestimates data.

4. Experimental procedure

4.1. Fabrication of glass samples

Glasses with molar sodium concentrations ranging between 14 and 35% and with K ($[SiO_2]/[B_2O_3]$) approximately 2.5 and 4.5 have been perpetrated. Silica, orthoboric acid (H_3BO_3) and sodium carbonate (Na_2CO_3) powders were manually homogenized and put in a platinum/gold crucible for the elaboration. The furnace's temperature was first maintained at 200 °C for 2 h to dehydrate the orthoboric acid. Then the temperature was increased from 200 °C to 800 °C to ensure decarbonatation of the sodium carbonate and avoid bubbles and increased again between 1100 °C and 1300 °C for 3 h depending on the glass composition. The melt was removed from the furnace at high temperature and poured into a preheated carbon crucible. The crucible temperature was around the glass transition point (600 °C). Subsequently the glass melt was placed in a second furnace and cooled at a slower rate (10 °C/h) to release the residual stresses.

To verify the chemical composition a third party (PrimeVerre) has been hired to conduct the chemical analysis. Sample verification was carried out via SEM–EDS (Environmental Electronic microscope coupled with an Energy Dispersive Spectrometer) and/or ICP-AES (Inductively coupled plasma atomic emission spectroscopy). SEM–EDS results revealed small amounts of impurities, less than 0.5%. Results reported herein are from the ICP-AES measurements (Table 3) and have an uncertainty of 10%. Thus fabricated glasses are within the range of our target values.

4.2. Density measurements

The densities were measured at 24 °C using a hydrostatic balance based on Archimedes' principle. First measure the specific gravity (SG) of the glass samples by weighting the sample in air, m_d, and water,

m_w. Then by multiplying by the density of water, ρ_w, one can arrive at the density of the sample, ρ_g:

$$\rho_g = SG * \rho_w = \frac{m_d}{m_d - m_w}(\rho_w) \tag{15}$$

This process was repeated 5 times. Results herein are the averages of these 5 measurements.

5. Simulation procedures

Using molecular dynamics (MD) simulations one can gain access to the basic structural building blocks of ternary SiO_2–B_2O_3–Na_2O (SBN) glass systems. MD simulations are performed on SBN systems, using the empirical interatomic potential developed by Kieu et al. [48]. This potential incorporates the Buckingham potential with Coulomb interactions via an Ewald sum. Guillot–Sator potential parameters have been used to describe the Si–O, Na–O and O–O interactions. The parameters of the B–O interactions have been adjusted to fit density and elastic modulus properties on a large set of SiO_2–B_2O_3–Na_2O glasses. All the calculations are performed with the DLPOLY code [55].

Initially independent cubical systems of 10,000 randomly placed Si, B, O, and Na atoms were prepared and equilibrated for 1 ns (time step was 1 fs) at 5000 K with a density 5% lower than the experimental density. Subsequently the systems are cooled to 300 K via a cooling process at a quench rate equal to 2×10^{12} K/s. Then the equilibrium volume at ambient temperature is determined by an NPT calculation (10^6 time steps). Finally, the structure is equilibrated in the NVE ensemble during 10^6 time steps using the equilibrium volume determined previously. This process is repeated for all compositions presented in Table 3 plus 2 extra compositions: SBN15 ($57.63\%SiO_2$–$15.2\%Na_2O$–$27.13\%B_2O_3$) and SBN40 ($38.8\%SiO_2$–$40\%Na_2O$–$21.2\%B_2O_3$). Structural analysis is done using 2400 different configurations taken during the final equilibration in the NVE ensemble. The delay between two successive configurations is equal to 400 time steps. These systems are used to gain access to the volume of the basic building blocks (f_1, f_2... and Q_4, Q_3...) of ternary SiO_2–B_2O_3–Na_2O glasses as detailed in the previous section.

The volume of these different units has been calculated via Voronoi cells. The following method is applied: in the first step the Voronoi volumes of all the atoms in a particular atomistic configuration are calculated. Then the different local groups listed previously are identified in the atomistic configuration by considering the first neighbors of all the atoms. A network former plus an oxygen (F–O) pair is considered as first neighbors if the F–O distance is lower than the cut-off radius depending on the F type. The cut-off radii are 2.1 Å and 2.0 Å for Si and B atoms respectively. For the oxygen atoms, we have distinguished

Table 3
Target molar composition of glasses and molar compositions of fabricated glass samples as measured from ICP-AES. It should be noted that ICP-AES methods have an uncertainty of 10%.

Name	Target & MD simulations			Measured via ICP-AES		
	SiO_2	Na_2O	B_2O_3	SiO_2	Na_2O	B_2O_3
SBN14	67.73	14.2	18.04	70	14.2	15.8
SBN12	59.66	12.2	28.17	59.6	16.5	23.9
SBN25	50.76	25.4	23.89	52.6	26.8	20.6
SBN30	47.33	30.4	22.28	51	28.9	20.1
SBN35	43.95	35.4	20.63	46.9	34.5	18.6
SBN59	59.24	25	15.76	61.13	25.5	13.3
SBN55	55.3	30	14.71	58.05	29.1	12.9

bridging and non-bridging ones. An oxygen atom is considered as bridging if it has two or more Si or B atoms in a first neighbor position. An oxygen atom is considered non-bridging if it has one or less Si or B atoms in a first neighbor position. So, every oxygen atom can be classified as bridging or non-bridging. No loose O atoms are detected. Some three coordinated O atoms are observed in some glassy compositions but the [3]O percentage never exceeds 2.13%.

Concerning the Na atoms, it is not possible to separate which atoms are in a charge compensating role around BO_4 groups, or in a modifying role near a non-bridging oxygen atom. So, in order to measure the volume of a local group containing Na atoms, the Voronoi volume of the Na atoms is defined as the average of the Voronoi volumes of all the Na atoms.

For a specific local group, its local volume is defined by the following equation:

$$V_{unit} = V^V(F) + \frac{1}{2}\sum_i^{BO} V^V(BO) + \sum_j^{NBO} V^V(NBO) + N_{Na} * V_{avg}(Na) \qquad (16)$$

where $V^V(F)$ is the Voronoi volume of the network former (Si or B atom) in the group. $V^V(BO)$ is the Voronoi volume of the bridging oxygen atoms, considered individually, and the sum is over all of the bridging oxygen atoms in a first neighbor position around the network former. It should be noted that the half exists because volume is associated to two network formers. $V^V(NBO)$ is the Voronoi volume of the NBO considered individually and the sum is over all of the NBOs in a first neighbor position around the network former. The last term corresponds to the N_{Na} sodium ions participating to the local group multiplied by the average Voronoi volume of the Na atoms (calculated considering all the Na atoms in the structural configuration).

For each configuration presented in Table 3, all f_i and Q_i are estimated along with their volume calculations. Moreover an average volume for each borate and silicate unit, V_{unit} can be estimated as follows

$$\langle V_{unit} \rangle = \frac{\sum_i^{SBN} f_i^{unit} * V_i^{unit}}{\sum_i^{SBN} f_i^{unit}} \qquad (17)$$

where the sum is over the different SBN compositions. f_i^{unit} corresponds to the fraction of the borate (f_i) or silicate (Q_i) unit of interest. V_i^{unit} corresponds to the volume of the borate or silicate unit of interest. This unit can be compared directly with fits previously postulated (Table 2).
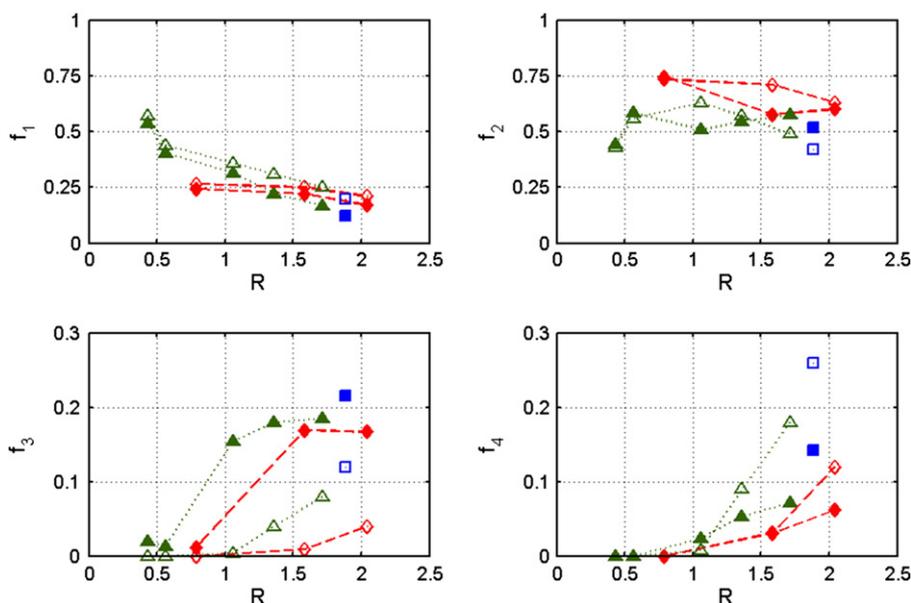
Table 5
K, R, R_{max} and R_{d1} for the glasses studied herein. The line marks the crossover from R less than R_{d1} to R greater than R_{d1}.

Glass	K	R	R_{max}	R_{d1}
SBN12	2.12	0.43	0.63	1.03
SBN14	3.76	0.79	0.74	1.44
SBN15	2.13	0.56	0.63	1.03
SBN25	2.12	1.06	0.63	1.03
SBN30	2.12	1.36	0.63	1.03
SBN35	2.13	1.72	0.63	1.03
SBN40	1.83	1.89	0.61	0.96
SBN59	3.75	1.58	0.73	1.44
SBN55	3.76	2.04	0.74	1.44

6. Results and discussion

6.1. Simulation results on the fraction of borate and silicate units

An advantage to MD simulations is that all the positions of the atoms are known. Thus the connectivity of the structure can be unveiled. Using the cutoffs presented in Section 5 the fraction of the different borate and silicate units can be estimated. Table 4 lists the % of molar mass of the systems simulated herein along with a direct count of the fraction of each structural unit. For comparison, the theoretical values (Eqs. (2) and (3)–(6)) for the fraction of each structural unit are presented for the target compositions (Table 4) and compositions as measured by ICS-AES (Appendix C: Table 10). In the region where $R < R_{d1}$ (Table 5), the fractions of borate and silicate units compare favorably with what is expected theoretically (Table 4 and Figs. 4 and 5). Afterwards, the quantity of sodium ions attaching to the borate network is larger than what is expected in theories. This has several ramifications. First the simulated f_2 faction is smaller than expected by theory (seen previously in simulations [50]) with the exception of high amounts of sodium (i.e. [Na$_2$O] ≳ 35); on the other hand, f_3 faction is substantially larger than expected by theory. Secondly, there is a readjustment of the other borate units due to the increase in sodium ions in the borate network and the increase in f_3 elements. Finally the simulated silicate network is less touched by the sodium ions than expected in theory as represented by the high Q_4 fraction. On the other hand, when sodium ions do enter the silicate network they have a tendency to isolate the Si atoms more, represented by an increase in the fraction of Q_2, Q_1, and Q_0 elements.

Table 4
The table is the fraction of borate and silicate units in MD simulations (gray rows) compared to the fraction of borate (Eqs. (3)–(6)) and silicate (Eq. (2)) units from theory for systems of interest (Table 3). Uncertainties in all fractions for MD simulations presented in the table are less than 0.001. Appendix C (Table 10) provides the fraction of borate and silicate units based on ICP-AES measurements.

|	Glass	SiO_2	Na_2O	B_2O_3	f_1	f_2	f_3	f_4	Q_4	Q_3	Q_2	Q_1	Q_0
$R<R_c$	SBN12	59.67%	12.20%	28.13%	0.57	0.43	0	0	1	0	0	0	0
					0.535	0.444	0.020	0	0.975	0.025	0	0	0
	SBN14	67.74%	14.25%	18.01%	0.265	0.735	0	0	0.97	0.03	0	0	0
					0.243	0.745	0.012	0	0.947	0.052	0	0	0
	SBN15	57.63%	15.25%	27.12%	0.44	0.56	0	0	1	0	0	0	0
					0.403	0.584	0.013	0	0.964	0.035	0.001	0	0
$R>R_c$	SBN25	50.74%	25.34%	23.91%	0.36	0.63	0.004	0.008	0.61	0.39	0	0	0
					0.314	0.508	0.154	0.024	0.767	0.201	0.030	0.001	0
	SBN30	47.35%	30.36%	22.29%	0.31	0.57	0.04	0.09	0.44	0.54	0.02	0	0
					0.222	0.546	0.180	0.053	0.671	0.279	0.045	0.005	0
	SBN35	43.92%	35.43%	20.65%	0.25	0.49	0.08	0.18	0.27	0.68	0.04	0	0
					0.168	0.574	0.185	0.072	0.546	0.340	0.100	0.012	0
	SBN40	38.78%	40.02%	21.21%	0.20	0.42	0.12	0.26	0.16	0.75	0.08	0	0
					0.121	0.520	0.216	0.142	0.394	0.409	0.165	0.027	0.005
	SBN59	59.22%	25%	15.78%	0.25	0.71	0.009	0.03	0.57	0.43	0	0	0
					0.222	0.577	0.169	0.031	0.701	0.255	0.040	0.003	0.001
	SBN55	55.30%	30.01%	14.69%	0.21	0.63	0.04	0.12	0.39	0.58	0.02	0	0
					0.169	0.602	0.167	0.062	0.596	0.312	0.077	0.014	0.001

Fig. 4. Pictorial representation of the borate unit fractions presented in Table 5: (top left) f_1; (top right) f_2; (bottom left) f_3; and (bottom right) f_4. Colors represent the K grouping: red diamonds $K \sim 3.75$; green triangles $K \sim 2.12$; and blue squares $K \sim 1.83$. Solid face markers depict simulation results; and open face markers depict theoretical results. The visualization of f_3 and f_4 units is enhanced by a zoom of the y-axis. Normally the axis ranges from 0 to 1. Lines connecting data point are for the eye.

Another aspect observed in simulations not considered in theory is NBO on the BO_4 elements. MD simulations do reveal that when $R < R_{d1}$ a small fraction of BO_4 units do have NBO (Table 7). However, as this number is small, neglecting it is not unreasonable. Yet when $R > R_{d1}$, the percent of BO_4 units with 1 or 2 NBOs swells to greater than 25% in the case of SBN35. The ramifications of this will become more evident in the following section on Voronoi volumes.

6.2. Voronoi volume elements from MD simulations

As stated above, MD simulations give access to the structure of various glasses atom-by-atom. Thus once the borate and silicate units have been identified elementary volume units are estimated via Voronoi volumes. Average results for each SBN glass are presented in Table 7. The volume of planar $BO_{3/2}$ groups (V_1) is somewhat smaller than what is expected for pure B_2O_3 and what is theorized by Inoue et al. [14], Feil and Feller [13], and Budhwani and Feller [12] fits. The origin of these differences could originate from the fact that B_2O_3's short range order is a planar $BO_{3/2}$ group. Thus extracting a volume from a plane is somewhat problematic. Yet Voronoi cells do give us an insight on what it could be. Another interesting observation is that V_1 has a tendency to decrease as [Na$_2$O] increases (Fig. 6a). Furthermore this decrease appears to be dependent on K. It is known that adding Na atoms to a silicate network leads to a decrease of the free volume of the glass structure because the alkali ions
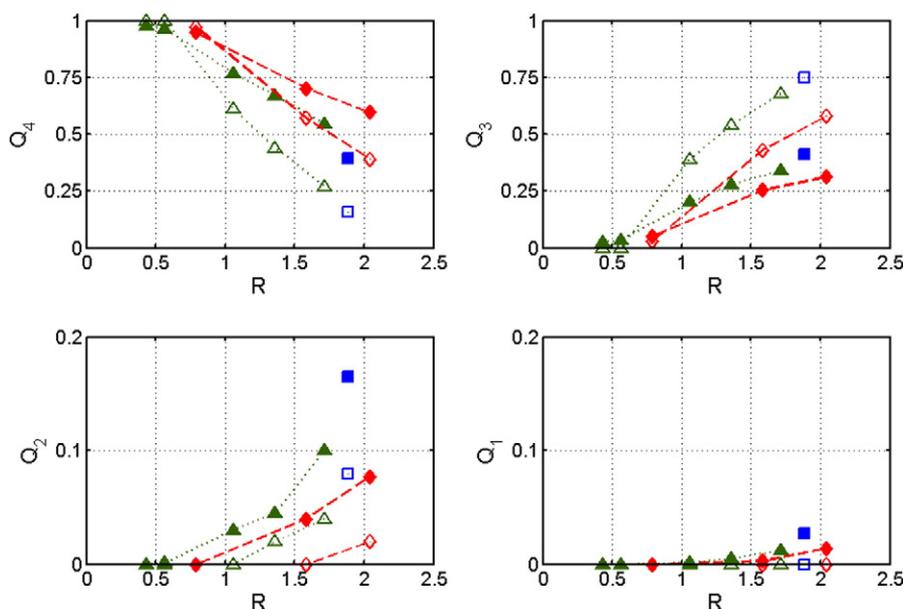
Fig. 5. Pictorial representation of the silicate unit fractions presented in Table 5: (top left) Q_4; (top right) Q_3; (bottom left) Q_2; and (bottom right) Q_1. Colors represent the K grouping: red diamonds $K \sim 3.75$; green triangles $K \sim 2.12$; and blue squares $K \sim 1.83$. Solid face markers depict simulation results; and open face markers depict theoretical results. The visualization of Q_2 and Q_1 units is enhanced by a zoom of the y-axis. Normally the axis ranges from 0 to 1. Lines connecting data point are for the eye.

Table 6

The percentage of BO_4 units bonded to 0, 1, and 2 NBOs. BO_4 units did not contain 3 and 4 NBOs.

Glass	0 NBO	1 NBO	2 NBOs
SBN14	98.37	1.63	0
SBN12	99.11	0.89	0
SBN15	98.55	1.45	0
SBN25	86.88	12.62	0.50
SBN30	81.57	17.68	0.75
SBN35	74.91	23.07	2.03
SBN59	81.37	17.72	0.91
SBN55	75.71	22.16	2.13

occupy the interstitial sites [56]. Subsequently the average Voronoi volumes of the other chemical elements mechanically decrease, explaining the trends observed on Fig. 7.
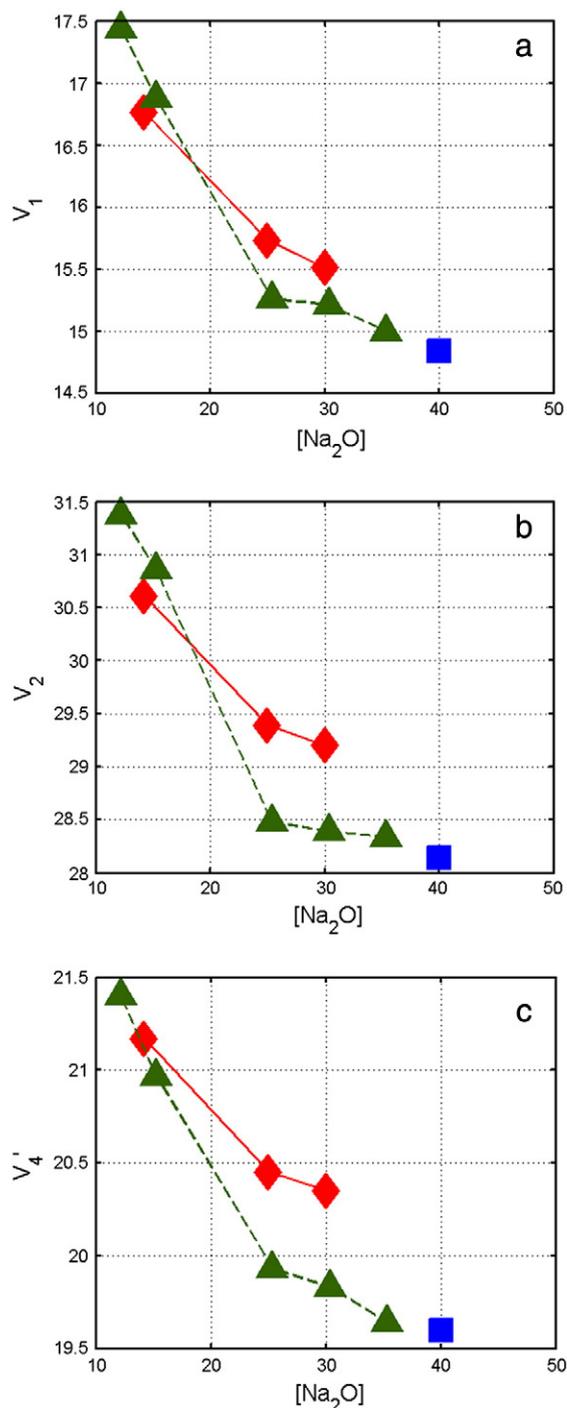
The unit volume of BO_4 groups (V_2) is larger than what is postulated by Inoue et al. and Dell et al. [10,14,28,29]; conversely, the volume of the silica tetrahedron (V'_4) is underestimated. There are several possibilities for this. The predominant effect is that again Na atoms reduce the amount of free volume in the glass structure. Secondly, theoretical studies group all BO_4 units (Tetraborate, diborate like, and Reedmergnerite like) together [10,14,28,29]; moreover, they exclude danburite-like units ($NA_2O\ B_2O_3\ 3SiO_2$) [51]. This grouping is problematic due to (1) variations in the B–B (i.e. 2.69 Å for a binary SiO_2-B_2O_3 glass with $K = 2.28$ and 2.8 Å for SBN14) and Si–B (i.e. 2.80 Å for a binary SiO_2-B_2O_3 with $K = 2.28$ and 2.91 Å for SBN14) bond lengths in lieu of sodium and in the presence of sodium [57]; and (2) broad asymmetrical pair correlation functions for the B–B and Si–B bond lengths [48,57]. Furthermore, NBO on the BO_4 units exists in simulations and they have been grouped with fully coordinated BO_4 units (Table 6). It is unclear as to whether this is an artifact of the simulations or factual. However, these NBOs and variations in BO_4 units undoubtedly lead to volume variations based on the number of NBO on the BO_4 units. Moreover as in the case of the planar $BO_{3/2}$ group, both V_2 and V'_4 appear to be inversely proportional to $[Na_2O]$ (Fig. 6b and c).

Metaborate (V_3), Pyroborate (V_4), and silica tetrahedrons with 1 NBO (V'_3) or 2 NBOs (V'_2) Voronoi volume units compare quite favorably with theoretical values. On the other hand, silica tetrahedrons with 3 NBOs (V'_1) or 4 NBOs (V'_0) Voronoi volume units do not compare favorably with theoretical values. This is substantially due to a lack of experimental data in which to derive theories from and the small fraction of these units in the MD simulations. On the other hand, Inoue et al. predict that V'_1 is the smallest of all the silicate units [14]. This is an unrealistic presumption considering that the V'_1 entity has 3 NBO and 3 Na^+ ions to compensate the local charge.

Fig. 6. Depicts the dependence of the volume of (a) the planar $BO_{3/2}$ group, f_1; (b) the BO_4 group, f_2; and (c) the Q_4 group versus the sodium concentration for MD simulations. Colors represent the K grouping: red diamonds $K \sim 3.75$; green triangles $K \sim 2.12$; and blue square $K \sim 1.83$. Lines connecting data points are for the eye. Clearly the volume of these structural units decreases with increasing sodium concentration. Also a dependence on K is evidenced.

Table 7

Elementary volume elements of the borate and silicate units extracted from MD simulations using Voronoi volumes for each glass. The units of which are cm^3/mol. The weighted average takes into consideration the fraction of each unit in the glasses. Inoue's values are shown for comparison.

Reference/ Name	Borate units				Silicate units				
	V_1	V_2	V_3	V_4	V'_4	V'_3	V'_2	V'_1	V'_0
Inoue et al. [14]	19.2	21.0	29.0	41.7	26.3	35.2	50.3	20.8	–
Weighted Average (MD)	16.17	29.53	30.63	44.88	20.60	35.73	50.29	65.40	78.99
SBN12	16.76	30.61	34.77	–	21.17	39.69	–	–	–
SBN14	17.44	31.38	35.69	–	21.40	39.96	60.46	–	–
SBN15	16.88	30.86	36.01	–	20.97	40.10	59.12	–	–
SBN25	15.26	28.48	30.99	46.14	19.93	35.66	51.29	67.10	–
SBN30	15.21	28.39	30.31	45.36	19.83	35.25	50.39	66.59	–
SBN35	15.00	28.34	29.88	44.65	19.64	34.82	49.74	64.76	78.74
SBN40	14.84	28.14	29.39	43.85	19.60	34.43	60.46	–	–
SBN59	15.73	29.39	31.39	46.78	20.45	36.41	52.14	67.95	81.40
SBN55	15.51	29.20	30.87	45.76	20.35	35.84	51.05	66.48	82.30

In general, all local volumes of borate units and Q_4, Q_3, and Q_2 silica units have a tendency to decrease when the Na_2O concentration increases. No correlation appears with the B_2O_3 concentration.

6.3. Comparison of experimental, simulation and theoretical results of ternary SiO_2–B_2O_3–Na_2O glass densities

Density results are presented in Table 8 and Figs. 7 and 8. Experimental (ρ_{exp}) and simulation (ρ_{sim}) results compare quite favorably with 0.3%
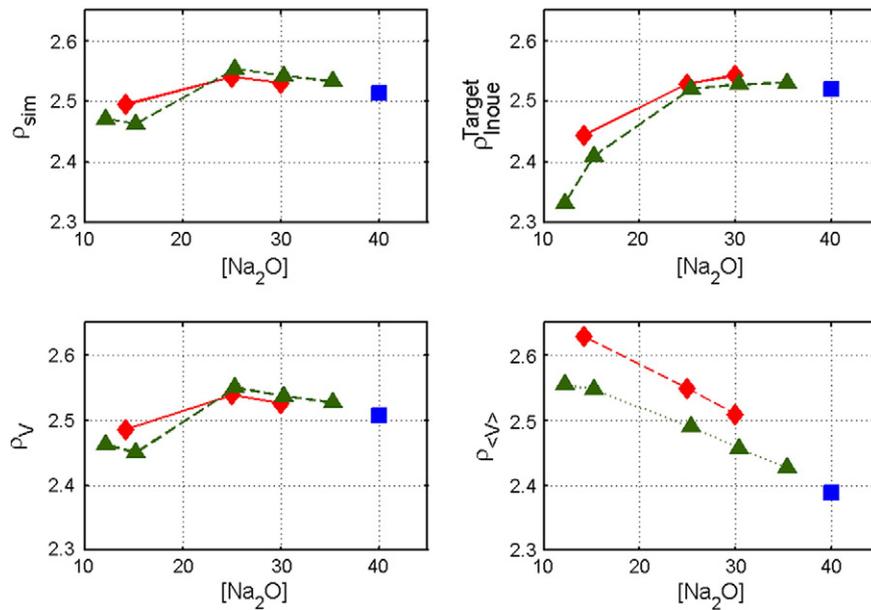
Fig. 7. Image of density results presented in Table 9 for target vales. Densities are obtained from: (top left) MD simulations (ρ_{sim}); (Top right) Inoue's equations for target densities (ρ_{Inoue}^{Target}); Voronoi volumes for extracting densities from each chemical composition (ρ_V); and Voronoi volumes for extracting densities the weighted average Voronoi volume ($\rho_{<V>}$).

Table 8
A comparison of densities obtained from experiments (ρ_{exp}), MD simulations (ρ_{sim}) and theory. Inoue's equations for target densities (ρ_{Inoue}^{Target}) and as measured ICP-AES densities ($\rho_{Inoue}^{ICP-AES}$) invoke the fraction of borate (Eqs. (3)–(6)) and silicate (Eq. (2)) units from theory along with Inoue's theoretical volumes (Table 7). Voronoi volumes for extracting densities from each chemical composition (ρ_V), and the weighted average Voronoi volume ($\rho_{<V>}$) invoke the fraction of borate and silicate units and Voronoi volumes estimated from simulations.

Name	Target values			ρ_{sim}	ρ_{Inoue}^{Target}	ρ_V	$(\rho_{(V)})$	Measured via ICP-AES			ρ_{exp}	$\rho_{Inoue}^{ICP-AES}$
	SiO2	Na2O	B2O3					SiO2	Na2O	B2O3		
SBN12	59.66	12.2	28.17	2.471	2.333	2.462	2.555	59.6	16.5	23.9	2.4619	2.452
SBN14	67.73	14.2	18.04	2.495	2.445	2.486	2.629	70	14.2	15.8	2.4736	2.449
SBN15	57.63	15.25	27.12	2.463	2.410	2.450	2.547					
SBN25	50.76	25.4	23.89	2.554	2.521	2.550	2.490	52.6	26.8	20.6	2.5446	2.527
SBN30	47.33	30.4	22.28	2.542	2.528	2.537	2.457	51	28.9	20.1	2.5407	2.530
SBN35	43.95	35.4	20.63	2.533	2.531	2.527	2.427	46.9	34.5	18.6	2.5368	2.537
SBN40	38.78	40.02	21.21	2.513	2.521	2.508	2.389					
SBN59	59.24	25	15.76	2.541	2.529	2.539	2.549	61.13	25.5	13.3	2.5344	2.535
SBN55	55.3	30	14.71	2.531	2.543	2.526	2.509	58.05	29.1	12.9	2.5383	2.545

difference. These results also compare favorably with density estimated by invoking Voronoi volumes from each chemical composition (ρ_V, less than 0.5% maximal error and on average 0.3% error). Both Inoue's (ρ_{Inoue}^{Target}) and weighted average Voronoi volume ($\rho_{<V>}$) give reasonable estimates for the densities studied herein (average % error is 1.2% and 3% and the maximal error of 5% and 6% respectively). However, these results are not nearly as precise as the MD simulations and chemical composition Voronoi volumes. Inoue's values do correspond better when using

chemical compositions measured via ICP-AES molar masses (% error 0.4% and maximal error of 1%).

A secondary observation is that the differences in the fractions and elementary volume units between theory and simulations are masked in the overall density measurements. Thus more precise experiments are needed to better determine the fractions and elementary volume units. A study of this caliber will have to include a secondary method to verify the chemical compositions of glasses; otherwise it is hard to pin point the exact causes of the discrepancies.

7. Conclusion

Theoretical fits to real data do provide a suitable first estimate for densities. On the other hand, MD simulations reveal that the local volumes of the borate and silicate units have a tendency to decrease when the Na_2O concentration increases; a point excluded from theoretical fits. This correlation is probably linked to the Na behavior in the silicate network. In fact, Na ions introduced in a homogeneous silicate network occupy interstitial free volumes, leading to a decrease of the average Voronoi volumes of the other chemical elements. Hence a decrease in the local volumes of the borate and silicate units arises when the Na_2O concentration increases.
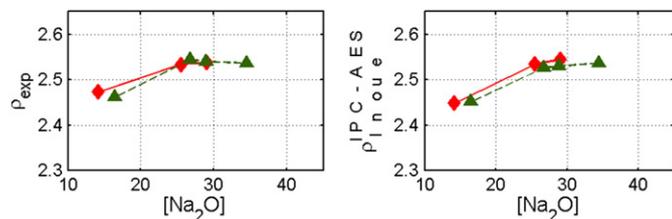

Fig. 8. Image of density results presented in Table 9 for as measured ICP-AES densities. Densities are obtained from: (left) experiments (ρ_{exp}) and Inoue's equations for target measured ICP-AES densities ($\rho_{Inoue}^{ICP-AES}$).

Herein the shifts between the densities are estimated directly, and the density estimated from the local volumes measured in the MD cells is always less than 0.3% and 0.5% with chemically dependent Voronoi volumes. Thus MD simulations give a better estimate of the densities than previous theories.

The fraction of f_1 and f_2 borate units for the different chemical compositions is globally coherent between the model and the MD simulations for $R < R_{d1}$. On the other hand the f_3 proportion is significantly larger and the f_4 proportion is smaller in the MD simulations than in the theoretical models. Another major difference between the simulations and theory is the percentage of Na_2O associating with the silica network after R_{d1} is lower than theorized. At this point in time we are unsure if this is an artifact of the potential or factual. More precise experiments are required to respond to this question.

Acknowledgments

Appendix A. Data

For the researcher's convenience, an up-to-date electronic version of the data can be found on the corresponding author's website.

[Na$_2$O]	[B$_2$O$_3$]	[SiO$_2$]	Density	Reference
0.35	0.19	0.47	2.5368	herein
0.29	0.20	0.51	2.5407	herein
0.27	0.21	0.53	2.5446	herein
0.29	0.13	0.58	2.5383	herein
0.17	0.24	0.60	2.4619	herein
0.26	0.13	0.61	2.5344	herein
0.20	0.17	0.63	2.5237	herein
0.14	0.16	0.70	2.4736	herein
0.00	1.00	0.00	1.83	[58]
0.20	0.50	0.30	2.4	[58]
0.10	0.46	0.44	2.181	[58]
0.06	0.48	0.46	2.12	[58]
0.04	0.49	0.47	2.06	[58]
0.09	0.45	0.47	2.162	[58]
0.03	0.49	0.48	2.069	[58]
0.00	0.45	0.55	1.97	[58]
0.00	0.31	0.70	2.042	[58]
0.00	0.00	1.00	2.2	[58]
0.00	0.00	1.00	2.212	[59]
0.78	0.22	0.00	2.34	[12]
0.76	0.24	0.00	2.39	[12]
0.75	0.25	0.00	2.39	[12]
0.73	0.27	0.00	2.39	[12]
0.71	0.29	0.00	2.38	[12]
0.69	0.31	0.00	2.39	[12]
0.67	0.33	0.00	2.39	[12]
0.63	0.37	0.00	2.39	[12]
0.57	0.43	0.00	2.36	[12]
0.46	0.54	0.00	2.37	[12]
0.44	0.56	0.00	2.39	[12]
0.41	0.59	0.00	2.37	[12]
0.41	0.59	0.00	2.38	[12]
0.38	0.63	0.00	2.37	[12]
0.33	0.67	0.00	2.37	[12]
0.29	0.71	0.00	2.32	[12]
0.23	0.77	0.00	2.25	[12]
0.20	0.80	0.00	2.19	[12]
0.17	0.83	0.00	2.14	[12]
0.13	0.87	0.00	2.11	[12]
0.13	0.87	0.00	2.13	[12]
0.09	0.91	0.00	2.04	[12]
0.07	0.93	0.00	2	[12]
0.07	0.93	0.00	2.03	[12]
0.05	0.95	0.00	1.92	[12]
0.00	1.00	0.00	1.82	[12]

Appendix A (continued)

[Na$_2$O]	[B$_2$O$_3$]	[SiO$_2$]	Density	Reference
0.70	0.20	0.10	2.46	[12]
0.63	0.25	0.13	2.42	[12]
0.56	0.29	0.15	2.43	[12]
0.64	0.18	0.18	2.48	[12]
0.44	0.37	0.19	2.43	[12]
0.60	0.20	0.20	2.47	[12]
0.56	0.22	0.22	2.46	[12]
0.62	0.15	0.23	2.51	[12]
0.29	0.48	0.24	2.45	[12]
0.58	0.17	0.25	2.49	[12]
0.50	0.25	0.25	2.45	[12]
0.25	0.50	0.25	2.41	[12]
0.21	0.53	0.26	2.35	[12]
0.55	0.18	0.27	2.5	[12]
0.43	0.29	0.29	2.47	[12]
0.12	0.59	0.29	2.16	[12]
0.50	0.20	0.30	2.48	[12]
0.00	0.67	0.33	1.91	[12]
0.44	0.22	0.33	2.49	[12]
0.33	0.33	0.33	2.48	[12]
0.33	0.33	0.33	2.5	[12]
0.55	0.11	0.34	2.53	[12]
0.26	0.37	0.37	2.47	[12]
0.50	0.13	0.38	2.52	[12]
0.38	0.25	0.38	2.5	[12]
0.20	0.40	0.40	2.41	[12]
0.17	0.42	0.42	2.37	[12]
0.50	0.07	0.43	2.52	[12]
0.43	0.14	0.43	2.51	[12]
0.29	0.29	0.43	2.5	[12]
0.13	0.43	0.43	2.27	[12]
0.33	0.22	0.44	2.5	[12]
0.33	0.22	0.44	2.51	[12]
0.38	0.15	0.46	2.51	[12]
0.07	0.47	0.47	2.11	[12]
0.22	0.31	0.47	2.47	[12]
0.25	0.25	0.50	2.51	[12]
0.25	0.25	0.50	2.52	[12]
0.17	0.33	0.50	2.4	[12]
0.00	0.50	0.50	1.98	[12]
0.14	0.34	0.52	2.33	[12]
0.19	0.27	0.54	2.49	[12]
0.27	0.18	0.55	2.51	[12]
0.07	0.37	0.56	2.17	[12]
0.33	0.10	0.57	2.52	[12]
0.29	0.14	0.57	2.52	[12]
0.14	0.29	0.57	2.43	[12]
0.20	0.20	0.60	2.51	[12]
0.23	0.15	0.62	2.52	[12]
0.24	0.11	0.65	2.51	[12]
0.17	0.17	0.67	2.5	[12]
0.11	0.22	0.67	2.45	[12]
0.09	0.18	0.73	2.37	[12]
0.13	0.13	0.75	2.43	[12]
0.20	0.35	0.45	2.451	[60]
0.17	0.38	0.45	2.404	[60]
0.15	0.40	0.45	2.343	[60]
0.13	0.42	0.45	2.294	[60]
0.11	0.44	0.45	2.245	[60]
0.09	0.46	0.45	2.197	[60]
0.07	0.48	0.45	2.167	[60]
0.05	0.50	0.45	2.144	[60]
0.00	1.00	0.00	1.84	[61–63]
0.00	0.75	0.25	1.905	[61,64]
0.00	0.30	0.70	2.055	[61,64]
0.00	0.20	0.80	2.11	[61,64]
0.00	0.15	0.85	2.134	[61,64]
0.00	0.10	0.90	2.143	[61,64]
0.00	0.05	0.95	2.182	[61,64]
0.30	0.55	0.15	2.441	[61,65]
0.20	0.65	0.15	2.244	[61,65]
0.17	0.68	0.15	2.148	[61,65]
0.145	0.705	0.15	2.085	[61,65]
0.10	0.75	0.15	2.002	[61,65]
0.07	0.78	0.15	1.942	[61,65]
0.05	0.80	0.15	1.883	[61,65]

Appendix A (continued)

[Na₂O]	[B₂O₃]	[SiO₂]	Density	Reference
0.03	0.82	0.15	1.834	[61,65]
0.00	0.85	0.15	1.779	[61,65]
0.30	0.05	0.65	2.537	[61,65]
0.25	0.10	0.65	2.507	[61,65]
0.20	0.15	0.65	2.462	[61,65]
0.15	0.20	0.65	2.345	[61,65]
0.05	0.30	0.65	2.105	[61,65]
0.01	0.34	0.65	2.035	[61,65]
0.00	0.00	1.00	2.2	[61,66]
0.00	1.00	0.00	1.843	[61]
0.00	0.95	0.05	1.853	[61]
0.00	0.90	0.10	1.864	[61]
0.00	0.80	0.20	1.89	[61]
0.00	0.70	0.30	1.92	[61]
0.00	0.65	0.35	1.935	[61]
0.00	0.60	0.40	1.951	[61]
0.00	0.55	0.45	1.968	[61]
0.00	0.50	0.50	1.985	[61]
0.00	0.45	0.55	2.002	[61]
0.00	0.40	0.60	2.02	[61]
0.30	0.65	0.05	2.356	[61,67]
0.25	0.70	0.05	2.283	[61,67]
0.10	0.85	0.05	2.039	[61,67]
0.30	0.60	0.10	2.393	[61,67]
0.25	0.65	0.10	2.319	[61,67]
0.20	0.70	0.10	2.216	[61,67]
0.10	0.80	0.10	2.052	[61,67]
0.30	0.55	0.15	2.421	[61,67]
0.25	0.60	0.15	2.351	[61,67]
0.20	0.65	0.15	2.252	[61,67]
0.10	0.75	0.15	2.065	[61,67]
0.30	0.50	0.20	2.448	[61,67]
0.25	0.55	0.20	2.378	[61,67]
0.20	0.60	0.20	2.282	[61,67]
0.10	0.70	0.20	2.094	[61,67]
0.30	0.45	0.25	2.473	[61,67]
0.25	0.50	0.25	2.416	[61,67]
0.20	0.55	0.25	2.33	[61,67]
0.10	0.65	0.25	2.118	[61,67]
0.30	0.40	0.30	2.492	[61,67]
0.20	0.50	0.30	2.331	[61,67]
0.10	0.60	0.30	2.133	[61,67]
0.30	0.35	0.35	2.513	[61,67]
0.20	0.45	0.35	2.389	[61,67]
0.10	0.55	0.35	2.145	[61,67]
0.30	0.30	0.40	2.529	[61,67]
0.20	0.40	0.40	2.419	[61,67]
0.10	0.50	0.40	2.164	[61,67]
0.30	0.25	0.45	2.553	[61,67]
0.20	0.35	0.45	2.445	[61,67]
0.10	0.45	0.45	2.182	[61,67]
0.30	0.20	0.50	2.543	[61,67]
0.20	0.30	0.50	2.478	[61,67]
0.10	0.40	0.50	2.211	[61,67]
0.30	0.15	0.55	2.539	[61,67]
0.20	0.25	0.55	2.512	[61,67]
0.10	0.35	0.55	2.239	[61,67]
0.30	0.10	0.60	2.54	[61,67]
0.20	0.20	0.60	2.525	[61,67]
0.10	0.30	0.60	2.264	[61,67]
0.30	0.05	0.65	2.52	[61,67]
0.10	0.25	0.65	2.292	[61,67]
0.20	0.10	0.70	2.502	[61,67]
0.10	0.20	0.70	2.326	[61,67]
0.20	0.05	0.75	2.447	[61,67]
0.10	0.15	0.75	2.357	[61,67]
0.10	0.10	0.80	2.37	[61,67]
0.30	0.70	0.00	2.34	[67]
0.25	0.75	0.00	2.27	[67]
0.20	0.80	0.00	2.18	[67]
0.15	0.85	0.00	2.11	[67]
0.10	0.90	0.00	2.04	[67]
0.05	0.95	0.00	1.94	[67]
0.00	1.00	0.00	1.78	[67]
0.20	0.75	0.05	2.202	[67]
0.00	0.95	0.05	1.857	[67]
0.00	0.90	0.10	1.868	[67]

Appendix A (continued)

[Na₂O]	[B₂O₃]	[SiO₂]	Density	Reference
0.00	0.85	0.15	1.873	[67]
0.00	0.80	0.20	1.879	[67]
0.00	0.75	0.25	1.888	[67]
0.00	0.70	0.30	1.898	[67]
0.00	0.65	0.35	1.936	[67]
0.00	0.60	0.40	1.953	[67]
0.45	0.00	0.55	2.502	[67]
0.40	0.00	0.60	2.536	[67]
0.35	0.00	0.65	2.559	[67]
0.20	0.15	0.65	2.521	[67]
0.30	0.00	0.70	2.484	[67]
0.25	0.00	0.75	2.438	[67]
0.20	0.00	0.80	2.388	[67]
0.00	0.00	1.00	2.217	[67]
0.00	1.00	0.00	1.844	[64]
0.00	0.90	0.10	1.865	[64]
0.00	0.50	0.50	1.99	[64]
0.39	0.30	0.30	2.56	[68]
0.38	0.31	0.31	2.561	[68]
0.33	0.33	0.33	2.536	[68]
0.31	0.34	0.34	2.518	[68]
0.26	0.37	0.37	2.499	[68]
0.23	0.38	0.38	2.48	[68]
0.22	0.39	0.39	2.449	[68]
0.20	0.40	0.40	2.429	[68]
0.18	0.41	0.41	2.389	[68]
0.167	0.417	0.417	2.35	[68]
0.149	0.426	0.426	2.311	[68]
0.13	0.435	0.435	2.261	[68]
0.09	0.455	0.455	2.161	[68]
0.30	0.23	0.47	2.526	[68]
0.29	0.24	0.48	2.521	[68]
0.03	0.48	0.48	2.045	[68]
0.27	0.24	0.49	2.518	[68]
0.25	0.25	0.50	2.53	[68]
0.23	0.26	0.51	2.517	[68]
0.19	0.27	0.54	2.48	[68]
0.18	0.27	0.55	2.471	[68]
0.17	0.28	0.56	2.45	[68]
0.15	0.28	0.56	2.43	[68]
0.14	0.29	0.57	2.396	[68]
0.13	0.29	0.58	2.366	[68]
0.12	0.29	0.59	2.308	[68]
0.09	0.30	0.61	2.237	[68]
0.06	0.31	0.63	2.147	[68]
0.03	0.32	0.65	2.098	[68]
0.00	1.00	0.00	1.833	[69]

## Appendix B. Details of the binary Na₂O–SiO₂ glass fractions

Commonly it is assumed that low quantities of Na_2O will convert bridging oxygen atoms to NBO (i.e. $Q_4 \rightarrow Q_3$) in a sliding rule fashion:

$$\left. \begin{array}{l} Q_4 = -2J + 1 \\ Q_3 = 2J \\ Q_2 = Q_1 = Q_0 = 0 \end{array} \right\} J < 0.25 \qquad (18)$$

Table 9
Coefficients for Gaussian fits done by matlab's curve fitting toolbox. Best fits (Q_i^{Best}) are presented to show that continuity fits (Q_i^C) are within the bounds of the best fits' 95% confidence bounds. From henceforth continuity fits will be used.

	A	B	C
Q_4^{Best}	1.04 ± .09	−.16 ± 0.15	0.8 ± .11
Q_4^C	1.04	−0.19	0.8
Q_3^{Best}	.77 ± .02	1.04 ± 0.2	0.74 ± .04
Q_3^C	.77	1.02	0.79
Q_2	.71 ± .04	2.08 ± .04	0.79 ± .05
Q_1	.52 ± .05	2.94 ± .05	.8
Q_0	.91	3.91 ± .03	.8
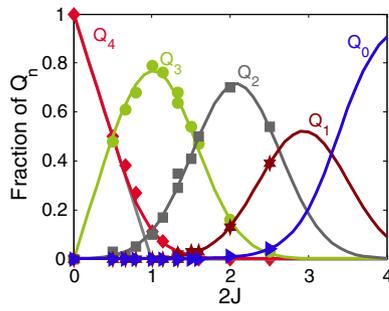
Fig. 9. Depicts fits developed herein to Maekawa et al.'s Si29 NMR data [40]: red diamonds: Q_4; green circles: Q_3; gray squares: Q_2; maroon stars: Q_1; and blue triangles: Q_1. As seen in the figure fits proposed herein reproduce data trends adequately.

Analyzing Maekawa et al.'s paper, this is approximately true until $J = 0.25$ corresponding to half the tetrahedra having Na^+ ions associated with them (Table 9) [40]. Eq. (18) can be used to estimate the annihilation of Q_4 units just until $J = 0.5$ after which $Q_4 = 0$. This fit is not perfect due to incomplete transformations and the formation of Q_2 (Fig. 9 dark gray line). Hence a better fit in this region ($0.25 < J < 0.5$) comes from:

$$Q_4 = Ae^{-\left(\frac{2J-B}{C}\right)^2}. \quad (19)$$

Combing the Eqs. (18) and (19) gives the best fit:

$$Q_4 = \begin{cases} -2J + 1 & J < .25 \\ Ae^{-\left(\frac{2J-B}{C}\right)^2} & J > .25 \end{cases} \quad (20)$$

It should be noted that the best fit leads to a discontinuity at $J = .25$. Thus parameters have been slightly adjusted to maintain continuity; however selected parameters are within the 95% confidence bounds as calculated by Matlab's curve fitting toolbox. A similar scenario occurs at $J = 0.25$ for Q_3. Q_2 has been fully fitted by Matlab's curve fitting toolbox and coefficients presented in Table 9 sufficiently model Maekawa et al.'s data (Fig. 9). For both Q_1 and Q_0, the data is rather insufficient for complete fits; hence several assumptions have been made. In the case of Q_1 the full width at half maximum (FWHM) has been set to 1.88 (implying $C = 0.8$). This choice was made as it was in agreement with the FWHMs of Q_4, Q_3, and Q_2. For Q_0, an assumption would be that the fraction of Q_0 would migrate to 1 as the sodium content increases. Hence a logistic function is the rational choice:

$$Q_0 = \frac{1}{1 + 2.2 * 10^5 e^{-3.65*(2J)}} \quad (21)$$

(Fig. 9 blue curve). This function has been fitted with Maekawa et al.'s data and a sudo point, $Q_0(J = 2) = 1 - \sum_{i=1}^{4} Q_i(J = 2)$.

Appendix C. Fraction of borate and silicate units based on ICP-AES results

References

[1] A. Grandjean, M. Malki, C. Simonnet, D. Manara, B. Penelon, Correlation between electrical conductivity, viscosity, and structure in borosilicate glass-forming melts, Phys. Rev. B Condens. Matter Mater. Phys. 75 (5) (2007) 054112 (http://link.aps.org/doi/10.1103/PhysRevB.75.054112).

[2] O.N. Koroleva, L.A. Shabunina, V.N. Bykov, Structure of borosilicate glass according to raman spectroscopy data, Glas. Ceram. 67 (11–12) (2011) 340–342.

[3] J. Windisch, F. Charles, E.M. Pierce, S.D. Burton, C.C. Bovaird, Deep-UV Raman spectroscopic analysis of structure and dissolution rates of silica-rich sodium borosilicate glasses, J. Non-Cryst. Solids 357 (10) (2011) 2170–2177.

[4] K. El-Egili, Infrared studies of Na₂O–B₂O₃–SiO₂ and Al₂O₃–Na₂O–B₂O₃–SiO₂ glasses, Physica B 325 (1-4) (2003)(PII S0921–4526(02)015747–8).

[5] D. Chen, H. Miyoshi, H. Masui, T. Akai, T. Yazawa, NMR study of structural changes of alkali borosilicate glasses with heat treatment, J. Non-Cryst. Solids 345 (2004) 104–107.

[6] L.S. Du, J.F. Stebbins, Site preference and Si/B mixing in mixed-alkali borosilicate glasses: a high-resolution B-11 and O-17 NMR study, Chem. Mater. 15 (20) (2003) 3913–3921.

[7] P.J. Bray, S.A. Feller, G.E. Jellison, Y.H. Yun, B-10 NMR-studies of the structure of borate glasses, J. Non-Cryst. Solids 38-9 (May 1980) 93–98.

[8] Y.H. Yun, P.J. Bray, Nuclear magnetic-resonance studies of glasses in system K₂O–B₂O₃–P₂O₅, J. Non-Cryst. Solids 30 (1) (1978) 45–60.

[9] Y.H. Yun, P.J. Bray, B-11 nuclear magnetic-resonance studies of Li₂O–B₂O₃ glasses of high Li₂O content, J. Non-Cryst. Solids 44 (2–3) (1981) 227–237.

[10] Y.H. Yun, S.A. Feller, P.J. Bray, Correction and addendum to nuclear magnetic-resonance studies of the glasses in the system Na₂O–B₂O₃–SiO₂, J. Non-Cryst. Solids 33 (2) (1979) 273–277.

[11] T. Nanba, M. Nishimura, Y. Miura, A theoretical interpretation of the chemical shift of Si-29 NMR peaks in alkali borosilicate glasses, Geochim. Cosmochim. Acta 68 (24) (2004) 5103–5111.

[12] K. Budhwani, S. Feller, Density model for the lithium, sodium and potassium borosilicate glass systems, Phys. Chem. Glasses 36 (4) (1995) 183–190.

[13] D. Feil, S. Feller, The density of sodium borosilicate glasses related to atomic arrangements, J. Non-Cryst. Solids 119 (1) (1990) 103–111.

[14] H. Inoue, A. Masuno, Y. Watanabe, K. Suzuki, T. Iseda, Direct calculation of the physical properties of sodium borosilicate glass from its chemical composition using the concept of structural units, J. Am. Ceram. Soc. 95 (1) (2012) 211–216.

[15] R.A. Golombeck, Investigations of Adsorption Sites on Oxide Surfaces Using Solid-State NMR and TPD-IGC, Ph.D. thesis Pennsylvania State University, 2008.

[16] G.N. Greaves, S. Sen, Inorganic glasses, glass-forming liquids and amorphizing solids, Adv. Phys. 56 (1) (2007) 1–166.

[17] H. Scholze, Glass: Nature, Structure, and Properties, Springer-Verlag, 1991.

[18] R.K. Kalia, A. Nakano, P. Vashishta, C.L. Rountree, L.V. Brutzel, S. Ogata, Multiresolution atomistic simulations of dynamic fracture in nanostructured ceramics and glasses, Int. J. Fract. 121 (1–2) (2003) 71–79.

[19] L.V. Brutzel, C.L. Rountree, R.K. Kalia, A. Nakano, P. Vashishta, Dynamic fracture mechanisms in nanostructured and amorphous silica glasses million-atom molecular dynamics simulations, in: S. Komarneni, J. Parker, R. Vaia, G. Lu, J. Matsushita (Eds.), Nanophase and Nanocomposite Materials IV, Vol. 703 of Mater. REs. Soc. Symp. P, Symposium on Nanophase and Nanocomposite Materials IV held at the 2001 MRS Fall Meeting, Boston, MA, Nov 26-29, 2001, 2002, pp. 117–122.

[20] C.L. Rountree, R.K. Kalia, E. Lidorikis, A. Nakano, L.V. Brutzel, P. Vashishta, Atomistic aspects of crack propagation in brittle materials: multimillion atom molecular dynamics simulations, Annu. Rev. Mater. Res. 32 (2002) 377–400.

[21] C.L. Rountree, D. Bonamy, D. Dalmas, S. Prades, R.K. Kalia, C. Guillot, E. Bouchaud, Fracture in glass via molecular dynamics simulations and atomic force microscopy experiments, Phys. Chem. Glasses B 51 (2) (2010) 127–132.

[22] C.L. Rountree, S. Prades, D. Bonamy, E. Bouchaud, R. Kalia, C. Guillot, A unified study of crack propagation in amorphous silica: using experiments and simulations, J. Alloy Compd. 434 (Sp. Iss. SI) (2007) 60–63.

[23] P. Vashishta, R.K. Kalia, J.P. Rino, I. Ebbsjo, Interaction potential for SiO₂ — a molecular-dynamics study of structural correlations, Phys. Rev. B 41 (17) (1990) 12197–12209.

[24] R.A. Barrioy, R. Kernerz, M. Micoulautz, G.G. Naumisyz, Evaluation of the concentration of boroxol rings in vitreous B₂O₃ by the stochastic matrix method, J. Phys. Condens. Matter 9 (1997) 9219–9234 (http://www.fisica.unam.mx/~naumis/index_archivos/jpc97barrio.pdf).

Table 10
There exists a difference in the target molar composition of glasses and in the molar compositions of fabricated glass samples as measured from ICP-AES. The fraction of borate (Eqs. (3)–(6)) and silicate (Eq. (2)) units are calculated from theory.

	Glass	SiO₂	Na₂O	B₂O₃	f_1	f_2	f_3	f_4	Q_4	Q_3	Q_2	Q_1	Q_0
ICP-AES results	SBN12	59.6%	16.5%	23.9%	0.34	0.66	0	0	0.97	0.03	0	0	0
	SBN14	70%	14.2%	15.8%	0.22	0.78	0	0	0.95	0.06	0	0	0
	SBN25	52.6%	26.8%	20.6%	0.32	0.63	0.16	0.04	0.55	0.45	0	0	0
	SBN30	51%	28.9%	20.1%	0.30	0.60	0.03	0.07	0.47	0.52	0.014	$1e^{-4}$	0
	SBN35	46.9%	34.5%	18.6%	0.23	0.52	0.07	0.18	0.28	0.67	0.04	$2e^{-4}$	$1e^{-4}$
	SBN59	61.13%	25.5%	13.3%	0.20	0.74	0.12	0.05	0.54	0.46	0	0	0
	SBN55	58.05%	29.1%	12.9%	0.17	0.68	0.03	0.12	0.40	0.57	0.02	$1e^{-4}$	0

[25] G. Ferlat, T. Charpentier, A.P. Seitsonen, A. Takada, M. Lazzeri, L. Cormier, G. Calas, F. Mauri, Boroxol rings in liquid and vitreous B_2O_3 from first principles, Phys. Rev. Lett. 101 (6) (2008) 065504.

[26] R.L. Mozzi, B.E. Warren, Structure of vitreous boron oxide, J. Appl. Crystallogr. 3 (1970) 251.

[27] J. Krogh-Moe, The crystal structure of a sodium triborate modification, beta-$Na_2O.3B_2O_3$, Acta Crystallogr. B B28 (1972) 1571–1576.

[28] P.J. Bray, A.E. Geissberger, F. Bucholtz, I.A. Harris, Glass structure, J. Non-Cryst. Solids 52 (1–3) (1982) 45–66.

[29] W.J. Dell, P.J. Bray, S.Z. Xiao, B-11 NMR-studies and structural modeling of Na_2O–B_2O_3–SiO_2 glasses of high soda content, J. Non-Cryst. Solids 58 (1) (1983) 1–16.

[30] J. Krogh-Moe, Crystal-structure of sodium diborate $Na_2O.2B_2O_3$, Acta Crystallogr. B 30 (Mar 15 1974) 578–582.

[31] D. Manara, A. Grandjean, D.R. Neuville, Structure of borosilicate glasses and melts: a revision of the Yun, Bray and Dell model, J. Non-Cryst. Solids 355 (50–51) (2009) 2528–2531.

[32] J. Krogh-Moe, Interpretation of the infra-red spectra of boron oxide and alkali borate glasses, Phys. Chem. Glasses 6 (1965) 46.

[33] T. Asahi, S. Nakayama, Y. Miura, T. Nanba, H. Yamashita, T. Maekawa, Preparation of Na_2S–B_2O_3–SiO_2 glass systems and local structure analysis, J. Ceram. Soc. Jpn. 114 (1332) (2006) 697–704 (https://www.jstage.jst.go.jp/article/jcersj/114/1332/114_1332_697/_pdf).

[34] G.H. Wolf, D.J. Durben, P.F. McMillan, High-pressure Raman spectroscopic study of sodium tetrasilicate ($Na_2Si_4O_9$) glass, J. Chem. Phys. 93 (4) (1990) 2280, http://dx.doi.org/10.1063/1.459007.

[35] P. McMillan, Structural studies of silicate glasses and melts — applications and limitations of Raman spectroscopy, Am. Mineral. 69 (1984) 622–644 (http://www.minsocam.org/ammin/am69_622.pdf).

[36] S.W. Martin, J.W. Mackenzie, A. Bhatnagar, S. Bhowmik, S.A. Feller, M.L. Royle, Si-29 mas nmr-study of the short-range order in sodium borosilicate glasses, Phys. Chem. Glasses 36 (2) (1995) 82–88.

[37] A.V. Loshagin, E.P. Sosnin, Boron-11, silicon-29, and sodium-23 NMR in sodium borosilicate glasses, Glass Phys. Chem. 20 (3) (1994) 250–258.

[38] P. Zhang, C. Dunlap, P. Florian, P.J. Grandinetti, I. Farnan, J.F. Stebbins, Silicon site distributions in an alkali silicate glass derived by two-dimensional Si-29 nuclear magnetic resonance, J. Non-Cryst. Solids 204 (3) (1996) 294–300.

[39] R. Martens, W. Muller-Warmuth, Structural groups and their mixing in borosilicate glasses of various compositions — an NMR study, J. Non-Cryst. Solids 265 (1–2) (2000) 167–175.

[40] H. Maekawa, T. Maekawa, K. Kawamura, T. Yokokawa, The structural groups of alkali silicate-glasses determined from Si-29 MAS-NMR, J. Non-Cryst. Solids 127 (1) (1991) 53–64.

[41] A.G. Clare, A.C. Wright, R.N. Sinclair, A comparison of the structural role of Na^+ network modifying cations in sodium silicate and sodium fluoroberyllate glasses, J. Non-Cryst. 213–214 (1997) 321–324.

[42] X.L. Yuan, A.N. Cormack, Local structures of MD-modeled vitreous silica and sodium silicate glasses, J. Non-Cryst. Solids 283 (1–3) (2001) 69–87.

[43] M. Fabian, P. Jovari, E. Svab, G. Meszaros, T. Proffen, E. Veress, Network structure of $0.7SiO(2)$–$0.3Na(2)O$ glass from neutron and x-ray diffraction and RMC modelling, J. Phys. Condens. Matter 19 (33) (2007) 335209.

[44] J. Du, A. Cormack, The medium range structure of sodium silicate glasses: a molecular dynamics simulation, J. Non-Cryst. Solids 349 (2004) 66–79, Glass Science for High Technology. 16th University Conference on Glass Science. http://www.sciencedirect.com/science/article/pii/S0022309304007963.

[45] H. Doweidar, Considerations on the structure and physical properties of B_2O_3–SiO_2 and GeO_2–SiO_2 glasses, J. Non-Cryst. Solids 357 (7) (2011) 1665–1670.

[46] L. van Wullen, G. Schwering, B-11-MQMAS and si-29–B-11 double-resonance NMR studies on the structure of binary B_2O_3–SiO_2 glasses, Solid State Nucl. Magn. Reson. 21 (3–4) (2002) 134–144.

[47] L.M. Wang, S.X. Wang, W.L. Gong, R.C. Ewing, W.J. Weber, Amorphization of ceramic materials by ion beam irradiation, Mater. Sci. Eng. A 253 (1-2) (1998)(Engn Fdn.).

[48] L.-H. Kieu, Compréhension de l'origine de l'évolution sous irradiation de la ténacité des verres nucléaires, (Ph.D. thesis) l'École Polytechnique, 2011.

[49] B.C. Bunker, D.R. Tallant, R.J. Kirkpatrick, G.L. Turner, Multinuclear nuclear-magnetic-resonance and Raman investigation of sodium borosilicate glass structures, Phys. Chem. Glasses 31 (1) (1990) 30–41.

[50] H. Inoue, A. Masuno, Y. Watanabe, Modeling of the structure of sodium borosilicate glasses using pair potentials, J. Phys. Chem. B 116 (40) (2012) 12325–12331 (http://apps.webofknowledge.com/full_record.do?product=UA&search_mode=CitingArticles&qid=4&SID=T2HeJNOfL5pHecHpakJ&page=1&doc=2).

[51] D. Manara, A. Grandjean, D.R. Neuville, Advances in understanding the structure of borosilicate glasses: a Raman spectroscopy study, Am. Mineral. 94 (5–6) (2009) 777–784.

[52] W.F. Du, K. Kuraoka, T. Akai, T. Yazawa, Study of Al_2O_3 effect on structural change and phase separation in Na_2O–B_2O_3–SiO_2 glass by NMR, J. Mater. Sci. 35 (19) (2000) 4865–4871.

[53] G. Eldamrawi, W. Mullerwarmuth, H. Doweidar, I.A. Gohar, Structure and heat-treatment effects of sodium borosilicate glasses as studied by Si-29 and B-11 NMR, J. Non-Cryst. Solids 146 (2-3) (1992) 137–144.

[54] S.H. Wang, J.F. Stebbins, On the structure of borosilicate glasses: a triple-quantum magic-angle spinning O-17 nuclear magnetic resonance study, J. Non-Cryst. Solids 231 (3) (1998) 286–290.

[55] W. Smith, M. Leslie, T. Forester, The dl_poly molecular simulation package, http://www.stfc.ac.uk/CSE/randd/ccg/software/DL_POLY/25526.aspx.

[56] A. Pedone, G. Malavasi, A.N. Cormack, U. Segre, M.C. Menziani, Insight into elastic properties of binary alkali silicate glasses; prediction and interpretation through atomistic simulation techniques, Chem. Mater. 19 (2007) 3144.

[57] L.-H. Kieu, J.-M. Delaye, L. Cormier, C. Stolz, Development of empirical potentials for sodium borosilicate glass systems, J. Non-Cryst. Solids 357 (18) (2011) 3313–3321 (http://www.sciencedirect.com/science/article/pii/S002230931100384X).

[58] A. Abd El-Moneim, Quantitative analysis of elastic moduli and structure of B_2O_3–SiO_2 and Na_2O–B_2O_3–SiO_2 glasses, Physica B 325 (2003) 1–4(PII S0921–4526(02)01545–4).

[59] R. Brückner, Properties and structure of vitreous silica, J. Non-Cryst. Solids 5 (2) (1970) 123–175.

[60] H. Doweidar, The density of sodium borosilicate glasses in relation to the microstructure, J. Phys. Chem. Solids 53 (6) (1992) 807–814.

[61] N.P. Bansal, R.H. Doremus, Handbook of Glass Properties, Academic Press Inc., 1986

[62] A. Cousen, W.E.S. Turner, A study of the glasses boric oxide–silica, J. Soc. Glas. Technol. 12 (1928) 169.

[63] R.R. Shaw, D.R. Uhlmann, Effect of phase separation on the properties of simple glasses. I. Density and molar volume, J. Non-Cryst. Solids 1 (6) (1969) 474–498.

[64] R. Jabra, J. Pelous, J. Phalippou, Brillouin scattering measurements of attenuation and velocity of hypersounds in SiO_2–B_2O_3 glasses, J. Non-Cryst. Solids 37 (3) (1980) 349–358.

[65] W.L. Konijnendijk, Structural differences between borosilicate and aluminosilicate glasses studied by Raman scattering, Glastech. Ber. 48 (10) (1975) 216–218.

[66] R.B. Sosman, The Properties of Silica: an Introduction to the Properties of Substances in the Solid Non-Conducting State, Book Department, The Chemical Catalog Company, Inc., New York, 1927. (http://lccn.loc.gov/28000585).

[67] M. Imaoka, H. Hasegawa, T. Hamaguchi, Y. Kurotaki, Chemical composition and tensile strength of glasses in the B_2O_3–PbO and B_2O_3–SiO_2–Na_2O systems, Yogyo Kyokai Shi 5 (1971) 164–172 (https://www.jstage.jst.go.jp/article/jcersj1950/79/909/79_909_164/_pdf).

[68] K. Takahashi, A. Osaka, R. Furuno, The elastic properties of the glasses in the system R_2O–B_2O_3–SiO_2 (R = Na and K) and Na_2O–B_2O_3, Yogyo Kyokai Shi 91 (1983) 199 (https://www.jstage.jst.go.jp/article/jcersj1950/91/1053/91_1053_199/_pdf).

[69] K. Vedam, W.C. Schneider, Variation of the refractive index of boric oxide glasses with hydrostatic pressure to 7 kbar, J. Appl. Phys. 43 (9) (1972) 3623–3627.